

Effect of La³⁺ and Ba²⁺ Substitution on Structural and Electrical Properties of Charge Ordered Divalent-Doped Sm_{0.5}Ca_{0.5}MnO₃ Manganite

Nuraina Hanum AbdulRuhim¹, Rozilah Rajmi^{1,*}, Muhammad Zulharmi Taqzim Kamaruzzaman¹, Norazila Ibrahim², Muhamad Kamil Yaakob²

¹Faculty of Applied Sciences, Universiti Teknologi MARA (UiTM), Perlis Branch, 02600, Arau, Perlis, Malaysia

²Faculty of Applied Sciences, Universiti Teknologi MARA (UiTM), 40450 Shah Alam, Selangor, Malaysia

*Corresponding Author's E-mail:rozilahrajmi@uitm.edu.my

Received: 24 March 2025 Accepted: 01 July 2025 Online First: 01 September 2025

ABSTRACT

The fascinating characteristics of mixed valence perovskite manganite, such as its colossal magnetoresistance and charge ordering, have drawn a lot of attention. Despite the continuous study, it is still difficult to modify the charge ordering and its structure by A-site substitution. Thus, this study addresses the problem of understanding the effect of A-site substitution with different cations on structural and electrical properties of manganite. Through this study, the solid-state reaction approach was used to synthesize the charge ordered $Sm_0 {}_5Ca_0 {}_5MnO_3$, $Sm_0 {}_2La_0 {}_3Ca_0 {}_5MnO_3$ and $Sm_0 {}_5Ca_0 {}_2Ba_0 {}_3MnO_3$ manganite. The structural and electrical properties of these materials were investigated. The single-phase, well-crystallized samples were all in an orthorhombic structure with a Pnma space group, according to the X-ray diffraction patterns. La³⁺ and Ba²⁺ substituted samples through Rietveld refinement show higher values of unit cell volume, indicating that the substitution at manganite's A-site was successful. According to Fourier transform infrared spectroscopy, the metal-oxygen and Mn-O bonds are visible at the 550 cm⁻¹ and 650 cm⁻¹ bands, respectively. While the fourpoint probe method was used to examine the impact of La^{3+} and Ba^{2+} electrical resistivity. Sm_{0.5}Ca_{0.5}MnO₃ and Sm_{0.5}Ca_{0.5}Ba_{0.3}MnO₃ manganite exhibit insulating properties in a temperature range of 30 K to 300 K, according to electrical resistivity measurements, while Sm₀,La₀,Ca₀,MnO₃





exhibits a metal-insulator transition. The magnetoresistance effect is demonstrated by the fact that all samples' resistivity was reduced by adding an external magnetic field of 0.8~T. The suppression of charge-ordered phase in $Sm_{0.2}La_{0.3}Ca_{0.5}MnO_3$, which is linked to increase in tolerance factor shows significant role and improved the double exchange mechanism. In $Sm_{0.5}Ca_{0.2}Ba_{0.3}MnO_3$, on the other hand, the weakening of charge-ordered phase is related to the A-site mismatch cation, which has bigger impact than high value of bandwidth and tolerance factor.

Keywords: Manganite; Charge Ordered; Structural; Electrical Resistivity; Magnetoresistance

INTRODUCTION

Mixed valence perovskite manganite in the form of $RE_{1-x}A_xMnO_3$ which RE is rare-earth trivalent ion (Sm^{3+} , La^{3+} and Pr^{3+}) while A is divalent (Ca^{2+} , Ba^{2+}), or monovalent ion (K^+ , Na^+) exhibit a few of the remarkable physical properties including colossal magnetoresistance (CMR), charge ordering (CO) metal-insulator transition and structure transformations [1]. Prior studies [2] suggest that the previous mentioned properties are due to Jahn-Teller (JT) interaction which promotes paramagnetic insulating behavior and the double exchange (DE) interaction that promotes ferromagnetic-metallic (FMM) states via an exchange between Mn^{3+} and Mn^{4+} . In addition, both JT and DE are among the mechanism that used to explain the magnetic and transport properties of manganite compound. Besides that, CMR has drawn interest precisely due to its enormous potential for implementation in a few technologies including spintronic, fuel cells and optical applications [3]. Between those properties, CO has piqued the interest of researchers in half-doped $RE_{0.5}A_{0.5}MnO_3$ as there are several records on these topics.

For this study $Sm_{0.5}Ca_{0.5}MnO_3$ manganite are chosen as the manganite exhibit strong insulating behavior with $T_{\rm CO} \sim 270~{\rm K}$ [4,5] due to the presence of strong charge ordered that localised charge carrier. There are a few properties that affect the crystal structure of manganite such as tolerance factor, τ that indicates degree of lattice mismatch between A-O layers and B-O layers, where it reflects the degree of deformation of MnO₆ octahedral [6]. As the mismatch between the A-O and B-O layers increases, the charge

ordered phase in doped manganite is strengthened. The CO state was then further affected by A-site disorder, σ^2 , since the mismatch in A-site cation size leads to the formation of random lattice distortion, which in turn affects local lattice distortion in MnO₆ [7,8]. Study on Sm_{0.5}Ca_{0.5}MnO₃ is very interesting due to its characteristic of having strong lattice distortion than other compounds such as La_{0.5}Ca_{0.5}MnO₃ [9,10] and Pr_{0.75}Na_{0.25}MnO₃ [11].

In addition, substitution of other rare-earth ion at A-site of manganite also has gathered a few studies and are very interesting. Additionally, the substitution of RE³+ at A-site able to maintain the ratio Mn³+/Mn⁴+ equal (1:1), but it is believed to alter the average ionic radius at A-site [12]. This can be proved by a few studies as substitution of Pr³+ in La₀,67Ba₀,33MnO₃ [13] modified average A-site cationic radius, increase the polaron activation energy thus enhance the electronic localisation which increase the resistivity of manganite. Besides that, substitution of Nd³+ in Pr₀,67Sr₀,33MnO₃ manganite offers decreasing value of resistivity with increasing concentration of Nd and the metal-insulator temperature (TMI) shift toward higher temperature region. This behavior suggested due to delocalisation of charge carriers. Furthermore, few works on substitution of Tb, Gd and Eu on LaCaMnO₃ [14,15] also has been carried out and offer various outcome due to modification of average A-site cationic radius. Thus, more studies are required on the impact of RE³+ substitution at A-site of manganite.

According to previous research, it is suggested that inducement of FMM occurred by substitution of Ba²⁺ that have higher ionic radius at A-site of Pr_{0.5}Ca_{0.5-x}Ba_xMnO₃[16] manganite. Thus, substitution manage to weaken the CO state and change the lattice distortion. In contrast to earlier compound, a study of La_{0.5}Ca_{0.5-x}Ba_xMnO₃ [10] manganite was unable to produce FMM state and stabilized the CO state since the substitution prevented electron from hopping to its neighboring sites. This result suggests a complicated interaction between the tolerance factor and A-site disorder that need more research. Furthermore, despite earlier studies, the effect of Ba substitution on the CO state of Sm_{0.5}Ca_{0.5}MnO₃ remains unclear.

In this study, La³⁺ ion and Ba²⁺ ion with the same concentration of 0.30 were chosen to be substituted at Sm_{0.5}Ca_{0.5}MnO₃ manganite. This is due to various findings on the substitution of divalent ion and trivalent ion at A-site of manganite. Since it is uncertain how the substitution of La

and Ba at A-site of manganite alters the material properties, further study is needed to understand the underlying mechanism. Additionally, further report is needed for substitution of Ba²⁺ as well as La³⁺ in Sm_{0.5}Ca_{0.5}MnO₃ manganite. This study offers information regarding the effect of Ba²⁺ and La³⁺ substitution on structural and electrical properties of Sm_{0.5}Ca_{0.5}MnO₃ manganite. The magnetoresistance of all samples also has been calculated and discussed in this paper.

EXPERIMENTAL

 $Sm_{0.5}Ca_{0.5}MnO_3$, $Sm_{0.2}La_{0.3}Ca_{0.5}MnO_3$ and $Sm_{0.5}Ca_{0.2}Ba_{0.3}MnO_3$ manganites were synthesized using the solid-state reaction method by weighing stoichiometric amount of high purity (99%) of samarium oxide (Sm₂O₂), calcium carbonate (CaCO₂), barium carbonate (BaCO₂), lanthanum oxide (La₂O₃) and manganese oxide (MnO₂). These oxides were thoroughly mixed using a mortar and pestle through a grinding process for 2 hours. Then the mixture was calcined in a furnace through calcination in air at fixed temperature of 950 °C for 12 hours and this process was repeated for the second time to ensure more homogenous mixture. This mixture was pressed into pellet under a load of 5 tons and then sintered at 1050 °C for 24 hours to ensure phase purity and homogeneity. The crystal structure and phase composition of Sm_{0.5}Ca_{0.5}MnO₃, Sm_{0.2}La_{0.3}Ca_{0.5}MnO₃ and Sm_{0.5}Ca_{0.2}Ba_{0.3}MnO₃ manganite were investigated by X-ray diffraction (XRD). In addition, Rietveld Refinement was used to provide information on the unit cell size and lattice parameter of each sample. The functional group found in perovskite samples was directly probed using Fourier transform infrared spectroscopy (FTIR) using an FTIR-Raman Drift Nicolet 6700 in the 400 - 4000 cm⁻¹ range. Both samples were fully mixed with KBr in the form of powder prior to characterization. Next, electrical properties of Sm_{0.5}Ca_{0.5}MnO₃, Sm_{0.2}La_{0.3}Ca_{0.5}MnO₃ and Sm_{0.5}Ca_{0.2}Ba_{0.3}MnO₃ manganites were investigated by using standard four-point probe method technique as a function temperature (30 K-300 K) under 0 T and 0.8 T of external magnetic field.

RESULTS AND DISCUSSION

The XRD patterns for the manganites $Sm_{0.5}Ca_{0.5}MnO_3$, $Sm_{0.2}La_{0.3}Ca_{0.5}MnO_3$ and $Sm_{0.5}Ca_{0.2}Ba_{0.3}MnO_3$ are illustrated in Figure 1. The characterization process was carried out at room temperature to evaluate the structure and sample purity before being analyzed using the Rietveld refinement technique. It is shown that all of the peaks in the XRD patterns are clear, sharp and well defined, indicating that the samples are well crystallized and in single phase with no impurities. Hence, crystal structure of all samples was indexed using in an orthorhombic structure *Pnma* space group ($\alpha=\beta=\gamma=90^{\circ}$). Through Rietveld refinement method, the orthorhombic structural results agree with prior studies [17] on $Sm_{0.5}Ca_{0.5}MnO_3$ manganite. This result also being supported with good fitness value (γ^2) of \sim 1 as tabulated in Table 1.

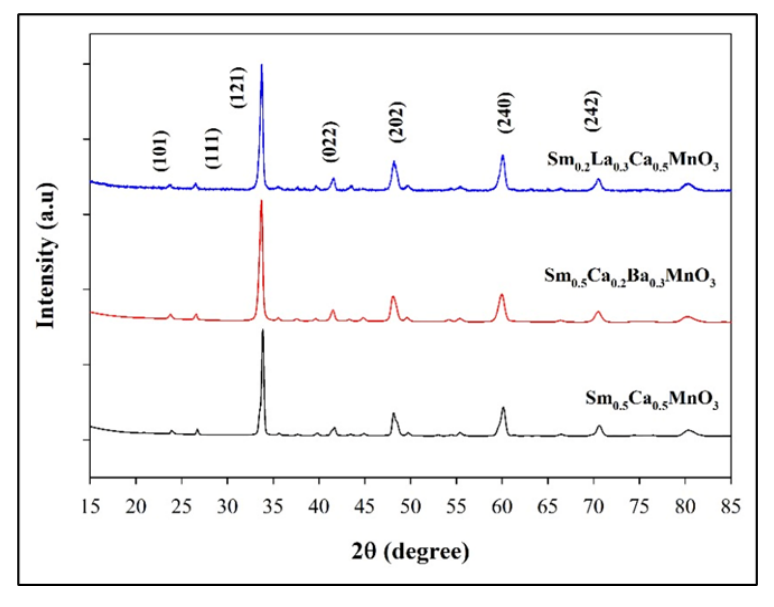


Figure 1: XRD patterns of $Sm_{0.5}Ca_{0.5}MnO_3$, $Sm_{0.5}Ca_{0.2}Ba_{0.3}MnO_3$ and $Sm_{0.2}La_{0.3}Ca_{0.5}MnO_3$ samples at room temperature.

Table 1: List of parameters acquired through Rietveld refinement; Bond length (Mn-O) and bond angle (Mn-O-Mn); Good fitness; Bandwidth; Average A-site ionic radius; Tolerance Factor and Variance of Sm_{0.5}C_{0.5}MnO₃, Sm_{0.7}La_{0.3}Ca_{0.5}MnO₃ and Sm_{0.5}Ba_{0.3}Ca_{0.5}MnO₃.

Sample	Sm _{0.5} Ca _{0.5} MnO ₃	Sm _{0.2} La _{0.3} Ca _{0.5} MnO ₃	Sm _{0.5} Ba _{0.3} Ca _{0.2} MnO ₃
Lattice parameter			
a (Å)	5.4043(5)	5.4411(7)	5.4215(8)
b (Å)	7.5459(8)	7.5969(2)	7.5637(6)
c (Å)	5.3540(4)	5.3958(9)	5.3817(2)
Volume, V (ų)	218.341(3)	222.310(7)	220.683(5)
Bond length			
Mn-O ₁ (Å)	1.948(9)	1.929(15)	1.937(19)
Mn-O ₂ (Å)	1.968(33)	1.969(22)	1.970(6)
< Mn-O > (Å)	1.958(21)	1.949 (19)	1.954(13)
Bond angle			
Mn-O ₁ -Mn (°)	156.20(25)	158.30(7)	157.00(4)
Mn-O ₂ -Mn (°)	155.10(14)	157.10(7)	156.20(27)
<mn-o-mn> (°)</mn-o-mn>	148.05(20)	157.70(7)	156.60(16)
Good fitness, χ ²	1.0700	1.7280	1.2540
Bandwidth, w (10 ⁻²)	9.1257	9.4925	9.3895
Average ionic radius, <r<sub>A> (Å)</r<sub>	1.1560	1.1812	1.2140
Tolerance factor, τ (nm)	0.9094	0.9183	0.9300
Variance, σ²(x10-²Å²)	0.0006	0.0090	0.0095

The final refinement value of lattice parameters obtained through Rietveld refinement are computed and tabulated in Table 1. For $Sm_{0.5}C_{0.5}MnO_3$, the volume of manganite recorded a 218.341 ų which closely similar to value of earlier research [18]. While with substitution of La^{3+} and Ba^{2+} , the volume of manganite shows an increasing value of 222.310 ų and 220.683 ų, respectively. The increasing value is believed due to substitution of larger ionic radius La^{3+} (r=1.216 Å) [14] into Sm^{3+} (r=1.07 Å) [19], Ba^{2+} (r=1.34 Å) [20] into Ca^{2+} (r=0.99 Å) [21] ion site which caused the

cell volume to expand, thus agree with earlier research [22]. This finding shows the successful substitution of La³+ and Ba²+ into Sm₀, Ca₀, MnO₃ manganite. Besides that, Mn-O bond angle as well as average ionic radius, <ra>h for both Sm₀, La₀, Ca₀, MnO₃ and Sm₀, Ca₀, Ba₀, MnO₃ shows increasing value from undoped sample. Modification in <ra>h proposed to affect the MnO₆ octahedral distortion and Mn-O-Mn angle (Table 1), thereby facilitate electron hopping and delocalization of charge carrier. In addition, tolerance factor has been calculated and tabulated, thus shows Ba²+ substitution record highest value followed by La³+ substitution. The increasement in tolerance factor suggested that the lattice mismatch between A-O and B-O layers decrease, thus reduced the MnO₆ mismatch. The decreasing of MnO₆ mismatch improve the Mn-O-Mn bond hence promote electron hopping. Table 1 also shows the value of electron bandwidth that has been calculated as described in Eq. (1).

$$w = \cos\frac{1}{2}(\pi - \gamma)/(d_{MN-O})^{3.5} \tag{1}$$

which, γ is the <Mn-O-Mn> bond angle, d(Mn-O) is the < Mn-O > length. Bandwith for both Sm_{0.2}La_{0.3}Ca_{0.5}MnO₃ and Sm_{0.5}Ca_{0.2}Ba_{0.3}MnO₃ record high value than pure sample, thus suggested the enhancement of the exchange coupling of Mn³⁺-Mn⁴⁺ hence giving high possibility in suppressing CO state and decreasing resistivity of manganite.

FTIR spectra for Sm_{0.5}Ca_{0.5}MnO₃, Sm_{0.5}Ca_{0.2}Ba_{0.3}MnO₃ and Sm_{0.2}La_{0.3}Ca_{0.5}MnO₃ samples are illustrated in the wavenumber range of 400 to 2000 cm⁻¹ which is shown in Figure 2.

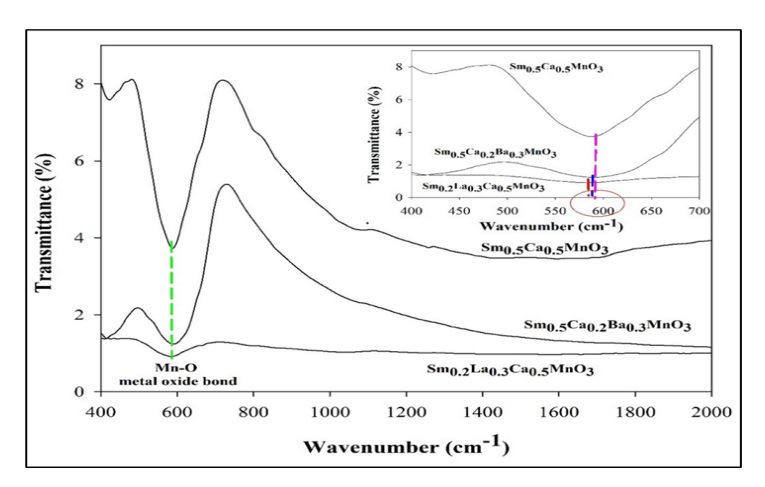


Figure 2: FTIR spectra for Sm_{0.5}Ca_{0.5}MnO₃, Sm_{0.2}La_{0.3}Ca_{0.5}MnO₃ and Sm_{0.5}Ca_{0.2}Ba_{0.3}MnO₃. The inset shows protuberant peak within wavenumber range of 500-600 cm⁻¹.

For all samples, it is observed that there are significant absorption bands appeared around the range of 500-650 cm⁻¹ which suggested due to Mn-O-Mn bonds. This finding aligns with previous study that suggested the protuberant peak exist due to Mn-O and O-Mn-O deformations and associated with MnO₆ octahedron [23,24]. Furthermore, based on the inset of Figure 2, the absorption peak band at the 550–650 cm⁻¹ range appears to move towards larger wavenumber values when La³⁺ and Ba²⁺ are substituted for Sm_{0.5}Ca_{0.5}MnO₃. The band that corresponds to the internal bending mode that relates to e_g-symmetry is likely the cause of this shift; hence, both bonds are related to the environment around MnO₆ octahedra [25]. In addition, the shifting towards higher wavenumber affect the DE mechanism that associated with e_g, electron and Mn-O-Mn bond and further discussed through electrical properties of manganite. The formation of Sm_{0.5}Ca_{0.2}Ba_{0.3}MnO₃ and Sm_{0.2}La_{0.3}Ca_{0.5}MnO₃ samples is confirmed by the spectra.

The Sm_{0.5}Ca_{0.5}MnO₃, Sm_{0.5}Ca_{0.2}Ba_{0.3}MnO₃ and Sm_{0.2}La_{0.3}Ca_{0.5}MnO₃ manganite samples' temperature dependency curved were investigated at temperature between 30 K and 300 K with an external magnetic field of 0 T and 0.8 T. Figure 3(a)-(c) illustrates the resistivity vs temperature (T) graphs for all samples under external magnetic field (H=0 T and H=0.8 T).

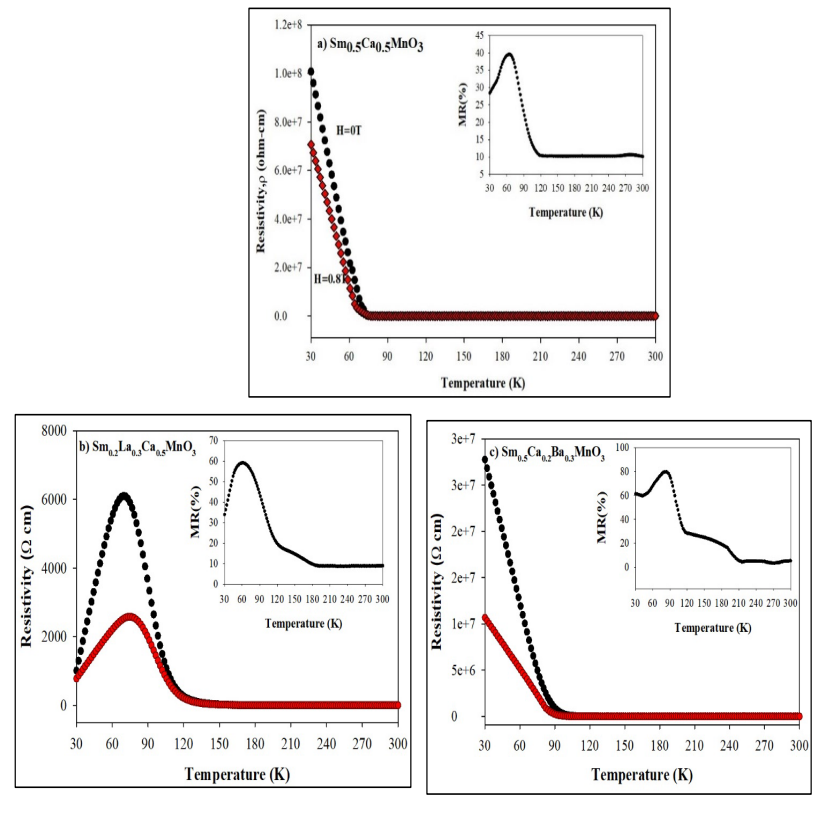


Figure 3(a)-(c): Resistivity curve of $Sm_{0.5}Ca_{0.5}MnO_3$, $Sm_{0.2}La_{0.3}Ca_{0.5}MnO_3$ and $Sm_{0.5}Ca_{0.2}Ba_{0.3}MnO_3$ manganite under 0 T (black) and 0.8 T(red). The inset in (a)-(c) shows MR(%) of $Sm_{0.5}Ca_{0.5}MnO_3$, $Sm_{0.2}La_{0.3}Ca_{0.5}MnO_3$ and $Sm_{0.5}Ca_{0.2}Ba_{0.3}MnO_3$ manganite.

Pure samples of $\rm Sm_{0.5} \rm Ca_{0.5} \rm MnO_3$ at H=0 T exhibit strong insulating behavior without insulator-metallic (MI) transition as temperature decreased. This insulating behavior also can be observed in $\rm Ba^{2+}$ substituted sample; however, the resistivity shows lower value than pure sample. It is suggested that substitution of $\rm Ba^{2+}$ weakens the CO state and reduce the resistivity even the substitution is unsuccessful to fully supress the strong CO state in manganite [26]. Generally, from previous study, substitution of larger ionic radius alter the $\rm Mn^{3+}\text{-}O\text{-}Mn^{4+}$ bond where it increases the tolerance factor that enhanced the electron hopping via DE. However, from Table 1 it is shown that σ^2 of $\rm Ba^{2+}$ recorded the highest value than $\rm La^{3+}$ -

substituted and pure sample hence indicating the probability of mismatch in size cation that enhanced the disorder. Therefore, it is proposed that the MnO₆ distortion, which is influenced by the degree of oxygen displacement and is connected to σ^2 , encourages charge carrier localisation, which leads to insulating behavior. In contrast to earlier research [27], the Ba²⁺substituted sample implies that the A-site mismatch cation appears to be more important in manganite than the bandwidth and tolerance factor values. In opposition, Figure 3(b) shows Sm_{0.2}La_{0.3}Ca_{0.5}MnO₃ successful induced MI transition where the T_{MI} are recorded at 69.59 K for H=0 T and increased (T_{MI} =74.99 K) with the existence of 0.8 T of magnetic field (Table 2). This finding, which is considered to be a result of La³⁺ substitute at Sm³⁺, appears to dominate over Ba²⁺ substitution, where the substitution may strengthen the DE process. The idea is consistent with previous research [14] that found that substituting a bigger RE³⁺ ion at the A-site suppresses CO and induces the FMM state. Besides that, the tolerance factor shows to be increased than pure sample which indicate that the La³⁺ substitution modifies the Mn³⁺-O-Mn⁴⁺ bond as well as MnO₆ octahedral distortion. This phenomenon improves the DE mechanism by increasing spin alignment. σ^2 that plays significant role in Ba²⁺-substituted sample likewise shows an increase value for Sm₀, La₀, Ca₀, MnO₃, indicating that the substitution has increased the disorder due to a mismatch in cation size. In contrast to Sm_{0.5}Ca_{0.2}Ba_{0.3}MnO₃, Sm_{0.2}La_{0.3}Ca_{0.5}MnO₃ is able to exhibit FMM behavior demonstrating the counterbalance impact of σ^2 and tolerance factor. This suggested that the tolerance factor for Sm_{0.2}La_{0.3}Ca_{0.5}MnO₃ which causes charge carrier delocalization, and DE enhancement is more prevalent than the A-site mismatch cation. This founding aligns with previous studies on $Pr_{0.6}Ca_{0.4-x}Ba_xMnO_3(x=0-0.30)$ [28] and $(La_{1-x}Pr_x)_{0.67}Ba_{0.33}MnO_3(x=0-0.30)$ [14].

Furthermore, red curve in Figure 3(a)-(c) indicate the resistivity curve under applied magnetic field of 0.8 T. It is observed that Sm_{0.5}Ca_{0.5}MnO₃, Sm_{0.5}Ca_{0.2}Ba_{0.3}MnO₃ and Sm_{0.2}La_{0.3}Ca_{0.5}MnO₃ manganite shows decreasing values of resistivity. While the inset of Figures 3(a)-(c) show the magnetoresistance curve of all samples, while magnetoresistance (MR) percentage at T=60 K are tabulated in Table 2 by using Eq. (2).

$$MR(\%) \frac{\rho(0,T) - \rho(H,T)}{\rho(0,T)} \times 100\%$$
 (2)

which resistivity value at 0 T indicate by $\rho(0,T)$ and resistivity value under applied magnetic field denoted by $\rho(H,T)$. At low temperatures, Sm_{0.5}Ca_{0.5}MnO₃ and Sm_{0.5}Ca_{0.2}BaO₃MnO₃ demonstrate MR peak which referred as extrinsic MR that is shown in the inset of Figures 3 (a) and (c). This type of MR is classified as spin-polarized tunneling (SPT) which occurs during electron transport across grain boundaries. Additionally, the uneven spin is aligned through supplying a weak magnetic field (H=0.8 T), which reduces the spin disorder, hence improved the spin alignment. Consequently, spin-polarization is created, which promotes spin scattering and decreases the resistance of a material [29,30]. H=0.8 T is still insufficient to suppress the CO state in in Sm_{0.5}Ca_{0.2}Ba_{0.3}MnO₃, even with the high percentage of MR listed in Table 2. While with the substitution of La³⁺, it is recorded that the MR percentage exhibit peak (Figure 3(b)) at the vicinity of T_{MI} (Table 2). The nature of this MR is different as MR which close to $T_{\rm MI}$ are known as intrinsic MR. Through intrinsic MR, the local spins are neatly aligned with existence of external magnetic field. Additionally, it is proposed that when SPT rises throughout the manganite, the frequency of itinerant electron transitioning from Mn³⁺ to Mn⁴⁺ increases in response to the applied magnetic field, leading to an enhancement of DE interaction. As a result, at 0.8 T, the resistivity dropped and the T_M moved toward a higher temperature and agrees with prior study that used slightly higher magnetic field [31].

Table 2: List of parameters; Metal-Insulator Temperature T_{MI;} Magnetoresistance at T=60 K.

Parameters	Sm _{0.5} Ca _{0.5} MnO ₃	Sm _{0.2} La _{0.3} Ca _{0.5} MnO ₃	Sm _{0.5} Ca _{0.2} Ba _{0.3} MnO ₃
T _{MI} (0 T) (K)	-	69.59	-
(0.8 T) (K)	-	74.99	-
MR (%) at T=60 K	39.25	59.09	68.51

CONCLUSION

In conclusion, $Sm_0 Ca_0 MnO_3$, $Sm_0 La_0 Ca_0 MnO_3$ and Sm_{0.5}Ca_{0.2}Ba_{0.3}MnO₃ were all categorised in *Pnma* space group through analysis by using Rietveld refinement method. With substitution of larger ionic radius such as La3+ and Ba2+ at A-site led to an observable increase in unit cell volume from 218.341 Å³ (Sm_{0.5}Ca_{0.5}MnO₃) to 220.683 Å³ $(Sm_{0.2}La_{0.3}Ca_{0.5}MnO_3)$ and 222.310 Å³ $(Sm_{0.5}Ca_{0.7}Ba_{0.3}MnO_3)$ indicating successful substitution. The increasing unit cell volume is consistent with results of past studies on manganite substitution. While through FTIR, the absorption band peak around the 550 - 650 cm⁻¹ thus offers information about the stretching vibration mode of Mn-O bond. In addition, the shift of absorption peak toward larger wavenumber with the substitution of La³⁺ and Ba²⁺ confirms the substitution effect on Sm_{0.5}Ca_{0.5}MnO₃. Both La³⁺ and Ba^{2+} substitution result in an enhancement in τ which associated with a reduction in MnO₄ octahedral distortion that improved the alignment of Mn-O-Mn angle. Furthermore, the < $r_{_{\rm A}}$ > also increased hence increasing the bandwidth, w which favors the FMM induction. However, only $Sm_0 La_0 Ca_0 MnO_3$ exhibit MI transition curve at $T_M = 69.59 K$, 74.99 K (0 T and 0.8 T) and able to induce FMM state, while Sm_{0.5}Ca_{0.2}Ba_{0.3}MnO₃ exhibit insulating behavior. This various outcome is believed due to the counterbalance effect between tolerance factor and A-site mismatch cation. For Sm₀,La₀,Ca₀,MnO₃, the tolerance factor plays more significant role thus enhance the DE mechanism and promote delocalization of charge carrier that allows electrons hopping. Our finding is consistent with previous studies, highlighting that the tolerance factor is crucial in inducing FMM state, thus allowing manganite exhibit mental-insulator behavior. On the other hand, A-site mismatch cation dominates Sm_{0.5}Ca_{0.2}Ba_{0.3}MnO₃, which causes MnO₆ to become distorted due to an increase of degree of oxygen displacement. This is related to σ^2 , which improves the localization of charge carriers. Besides that, both Sm_{0.5}Ca_{0.5}MnO₃ and Sm_{0.5}Ca_{0.2}Ba_{0.3}MnO₃ exhibit extrinsic MR while Sm₀, La₀, Ca₀, MnO₃ exhibit intrinsic MR that promotes delocalization of charge carrier resulting in decreasing of resistivity. Overall, the outcome from our study shows A-substitution able to change the structural, electron bandwidth and transport properties of manganite.

ACKNOWLEDGEMENTS

This work was funded by the Ministry of Higher Education (MOHE), Malaysia, and Universiti Teknologi MARA for supporting this project under Fundamental Research Grant Scheme (FRGS) (FRGS/1/2023/STG07/UITM/02/9).

REFERENCES

- [1] S. Panwar & I. Singh, 2020. A variational theory of magnetic susceptibility of Anderson lattice model: An application to colossal magnetoresistance manganites (Re_{1-x}A_xMnO₃), *Essence*, 20(11), SP2.129.
- [2] R. Rozilah, N. Ibrahim, S. Shamsuddin, S. Md Salleh & M. H. Othman, 2024. Effect of Pr³⁺ Substitution at the A-Site on the Structural and Electrical Properties of Hole-Doped La-Based Manganites, *Scientific Research Journal*, 21(1), 67 82.
- [3] S. Ye, J. Zhu, S. Zhu, Y. Zhao, M. Li, Z. Huang, H. Wang & J. He, 2023. Design strategies for perovskite-type high-entropy oxides with applications in optics, *ACS Applied Materials & Interfaces*, 15(40), 47475 47486.
- [4] M. Shah, M. Idrees, M. Nadeem, U. Ghazanfar, M. Atif, F.E. Alam, N. Asadullah, M.S. Irshad, M. Abbasi, F. Bukhari & M. Rizwan, 2022. Investigation of transport mechanism through charge-active regions in Sm_{0.5}Ca_{0.5}MnO₃, *Journal of Magnetism and Magnetic Materials*, 564, 170160.
- [5] H. Wang, H. Zhang, K. Su, S. Huang, W. Tan & D. Huo, 2020. Structure, charge ordering, and magnetic properties of perovskite Sm_{0.5}Ca_{0.5}MnO₃ manganite, *Journal of Materials Science: Materials in Electronics*, 31(1), 1 12.
- [6] N. Qin, Y. Pang, Z. Xu, X. Chen & J. Yan, 2023. Structural and thermoelectric properties of Gd_{2-2x}Sr_{1+2x}Mn₂O₇ Double-Layered

- manganites, Materials, 16(7), 2548.
- [7] M.A. Bally, F.A. Khan & M.A. Islam, 2019. Study of A-site disorder-dependent structural properties and magnetic ordering in polycrystalline perovskite Sm_{0.5}Ca_{0.5-x}Sr_xMnO₃, *Journal of Physics Communication*, 3(10), 105012.
- [8] S. Mollah, H. Huang, H. Yang, S. Pal, S. Taran & B. Chaudhuri, 2004. Non-adiabatic small-polaron hopping conduction in Pr_{0.65}Ca_{0.35-x} r_xMnO₃ perovskites above the metal-insulator transition temperature, Journal of Magnetism and Magnetic Materials, 284(1), 383 - 394.
- [9] N. Abate, J. Toro, G. Polla, I. Irurzun, S. Passanante, D. Vega, L. Granja & M. Quintero, 2023. Grain size effect on the critical behavior of the ferromagnetic transition in electronically phase separated La_{0.5}Ca_{0.5}MnO₃, *Ceramics International*, 49(24), 39945 39951.
- [10] V.N. Smolyaninova, S.E. Lofland, C. Hill, R.C. Budhani, Z.S. Gonen, B.W. Eichhorn & R.L. Greene, 2002. Effect of A-site cation disorder on charge ordering and ferromagnetism of La_{0.5}Ca_{0.5-y}Ba_yMnO₃, *Journal* of Magnetism and Magnetic Materials, 248(2), 348 - 354.
- [11] R. Rozilah, N. Ibrahim, Z. Mohamed, A. Yahya, N.A. Khan & M.N. Khan, 2017. Inducement of ferromagnetic-metallic phase in intermediate-doped charge-ordered Pr_{0.75}Na_{0.25}MnO₃ manganite by K⁺ substitution, *Physica B: Condensed Matter*, 521, 281 294.
- [12] G. Channagoudra, A.K. Saw, S. P. Rao & V. Dayal, 2020. Investigation of electronic and magneto-transport properties in Nd doped Pr_{0.67}Sr_{0.33}MnO₃ perovskite manganite, *AIP Conference Proceedings*, 2265(1), 030451.
- [13] M. Oumezzine, H.B. Sales, A. Selmi & E.K. Hlil, 2019. Pr³⁺ doping at the A-site of La_{0.67}Ba_{0.33}MnO₃ nanocrystalline material: assessment of the relationship between structural and physical properties and Bean–Rodbell model simulation of disorder effects, *RSC Advances*, 9(44), 25627 25637.

- [14] R.R. Doshi, P.S. Solanki, U. Khachar, D.G. Kuberkar, P.S.R. Krishna & A. Banerjee, P. Chaddah, 2011. First order paramagnetic—ferromagnetic phase transition in Tb³⁺ doped La_{0.5}Ca_{0.5}MnO₃ manganite, *Physica B*, 406(21), 4031 - 4034.
- [15] A. Krichene, W. Boujelben & A. Cheikhrouhou, 2013. Structural, magnetic and magnetocaloric properties in La_{0.5-x}Re_xCa_{0.5}MnO₃ manganites (x=0; 0.1 and Re=Gd, Eu and Dy), *Journal of Alloys and Compounds*, 550, 75 82.
- [16] B. Raveau, D. Zhu, A. Maignan, M. Hervieu, C. Martin, V. Hardy & S. Hébert. 2003. Sharp magnetization steps induced by A-site substitution in Pr_{0.5}Ca_{0.5}MnO₃, *Journal of Physics Condensed Matter*, 15(41),7055.
- [17] S.J. Huang, J.D. Liu, Z.W. Pan, H.J. Zhang & B.J. Ye, 2023. Effect of intrinsic vacancies on the electromagnetic properties of half-doped Sm_{0.5}Ca_{0.5}MnO₃ manganites studied by positron annihilation, *Journal of Applied Physics*, 134(6), 065104.
- [18] Y. Wang, H. Zhang, H. Wang, D. Yang, S. Huang, K. Su, W. Tan, & D. Huo, 2021. Charge ordering and magnetic properties of La_xSm_{0.5-x}Ca_{0.5}MnO₃ manganite, *Journal of Materials Science Materials in Electronics*, 32(14), 18721 18727.
- [19] V. Chauhan, P. K. Pandey, P. Dixit & P. C. Pandey, 2022. Structural and optical study of Sm³⁺ doped Ca₃(VO₄)₂ phosphors, *Materials Today Proceedings*, 67, 605 608.
- [20] C.P. Poole, H.A. Farach, R.J. Creswick & R. Prozorov, 2007. Cuprate crystallographic structures. *Superconductivity*, 195-229.
- [21] A. Hassen & P. Mandal, 2007. Correlation between structural, transport, and magnetic properties in Sm_{1-x}A_xMnO₃ (A=Sr,Ca), *Journal of Applied Physics*, 101(11), 113917.
- [22] S. Wang, J. Guo, R. Hou, L. Tian, H. Zhang, Q. Chen & Y. Li, 2024. Precise control of metal-insulator transition temperature in Lasubstituted La_{0.7}Ca_{0.3}MnO₃ via ionic radius tuning, *Journal of Alloys*

- and Compound, 1010, 177812.
- [23] I.S. Ismail, N.B. Mohamed, A. Hashim & Z. Mohamed, 2020. Effect of Bi Substitution on Structural and AC Magnetic Susceptibility Properties of Nd_{1-x}Bi_xMnO₃, *Crystals*, 10(6), 521.
- [24] M. Bourguiba, Z. Raddaoui, M. Chafra, & J. Dhahri, 2019. The investigation of structural and vibrational properties and optical behavior of Ti-doped La0.67Ba $_{0.25}$ Ca $_{0.08}$ Mn $_{1-x}$ Ti $_x$ O $_3$ (x = 0.00, 0.05 and 0.10) manganites, *RSC Advances*, 9(72), 42252 42261.
- [25] N.A. Azhar, U.R. Rosli, N.B. Mohamed, A. Hashim, & Z. Mohamed, 2021. A study on structural and physical properties of NdMnO₃ and Nd_{0.7}Ag_{0.3}MnO₃, *AIP Conference Proceedings*, 2368(1), 030007.
- [26] K. Ramya, S. Bharadwaj, S. Pola, G.S. Okram & Y. Kalyanalakshmi, 2024. Role of divalent doping at A-sites (A=Ca²⁺, Sr²⁺, Ba²⁺ & Pb²⁺) on thermoelectric and magnetoresistive properties in La_{0.67}(Bi_{0.0835}Na_{0.0835}) A_{0.165}MnO₃, *Journals of Alloys and Compound*, 1010, 177464.
- [27] N.A. Amaran & Z. Mohamed, 2023. Effect of 'A' and 'B' site substitution in Pr-based manganites: Fundamentals and main properties, *AIP Conference Proceedings*, 2720, 040028.
- [28] N. Ibrahim & A.K. Yahya, 2016. Inducement of itinerant electron transport in Charge-Ordered Pr_{0.6}Ca_{0.4}MnO₃ by Ba doping, *Journal of Superconductivity and Novel Magnetism*, 29(4), 911 922.
- [29] O. Vitayaya, P.Z.Z. Nehan, D.R. Munazat, M.T.E. Manawan & B. Kurniawan, 2024. Magnetoresistance (MR) properties of magnetic materials, *RSC Advances*, 14(26), 18617 18645.
- [30] N. Ibrahim, R. Rozilah, Z. Mohamed & A. Yahya, 2020. Magnetic and electronic transport properties of electron-doped La_{0.9-x}Bi_xTe_{0.1}MnO₃ (0.00≤x≤0.2) manganites, *Materials Chemistry and Physics*, 248,122940.

[31] X. Guan, H. Li, S. Jin, X. Yu, K. Chu, X. Pu & X. Liu, 2021. TCR and MR room-temperature enhancing mechanism of La_{0.7}K_{0.3}SrMnO₃ ceramics for uncooling infrared bolometers and magnetic sensor devices, *Ceramics International*, 47(13), 18931 - 18941.